

# cis-1,2-Aminohydroxylation of Alkenes Involving a Catalytic Cycle of Osmium(III) and Osmium(V) Centers: Os<sup>V</sup>(O)(NHTs) Active Oxidant with a Macrocyclic Tetradentate Ligand

Hideki Sugimoto,<sup>\*,†</sup> Akine Mikami,<sup>†</sup> Kenichiro Kai,<sup>†</sup> P. K. Sajith,<sup>‡</sup> Yoshihito Shiota,<sup>‡</sup> Kazunari Yoshizawa,<sup>\*,‡,§</sup> Kaori Asano,<sup>¶</sup> Takeyuki Suzuki,<sup>¶</sup> and Shinobu Itoh<sup>\*,†</sup>

<sup>†</sup>Department of Material and Life Science, Division of Advanced Science and Biotechnology, Graduate School of Engineering, Osaka University, 2-1 Yamadaoka, Suita, Osaka 565-0871, Japan

<sup>‡</sup>Institute for Materials Chemistry and Engineering and International Research Center for Molecular System, Kyushu University, 744 Motooka, Nishi-ku, Fukuoka 819-0395, Japan

<sup>§</sup>Elements Strategy Initiative for Catalysts & Batteries, Kyoto University, Nishi-ku, Kyoto 615-8520, Japan

<sup>¶</sup>Comprehensive Analysis Center, The Institute of Scientific and Industrial Research (ISIR), Osaka University, 8-1 Mihogaoka, Ibaraki, Osaka 567-0057, Japan

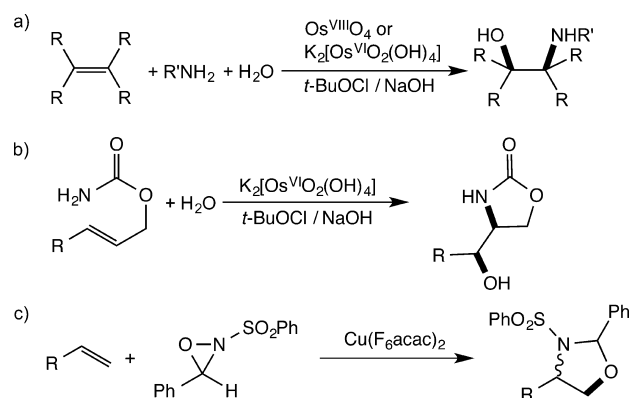
## Supporting Information

**ABSTRACT:** Catalytic activity of [Os<sup>III</sup>(OH)(H<sub>2</sub>O)(L-N<sub>4</sub>Me<sub>2</sub>)](PF<sub>6</sub>)<sub>2</sub> (**1**: L-N<sub>4</sub>Me<sub>2</sub> = N,N'-dimethyl-2,11-diaza-[3,3](2,6)pyridinophane) in 1,2-cis-aminohydroxylation of alkenes with sodium *N*-chloro-4-methylbenzenesulfonamide (chloramine-T) is explored. Simple alkenes as well as those containing several types of substituents are converted to the corresponding 1,2-aminoalcohols in modest to high yields. The aminoalcohol products have exclusively cis conformation with respect to the introduced -OH and -NHTs groups. The spectroscopic measurements including cold mass spectroscopic study of the reaction product of complex **1** and chloramine-T as well as density functional theory (DFT) calculations indicate that an oxido-aminato-osmium(V) species [Os<sup>V</sup>(O)(NHTs)(L-N<sub>4</sub>Me<sub>2</sub>)](PF<sub>6</sub>)<sub>2</sub> (**2**) is an active oxidant for the aminohydroxylation. The DFT calculations further indicate that the reaction involves a [3 + 2] cycloaddition between **2** and alkene, and the regioselectivity in the aminohydroxylation of unsymmetrical alkenes is determined by the orientation that bears less steric hindrance from the tosylamino group, which leads to the energetically more preferred product isomer.

## INTRODUCTION

The 1,2-aminoalcohol motif is frequently found in a wide range of natural products, biologically active molecules, and important intermediates in many organic syntheses.<sup>1–10</sup> The prevalence of this motif has inspired the development of numerous synthetic approaches to this structural unit and its derivatives.<sup>1,2</sup> Among them, the most powerful and generally utilized method is the direct 1,2-aminohydroxylation of alkenes using nitrenes as a nitrogen source, water molecule as a hydroxyl group source, and osmium tetroxide (Os<sup>VIII</sup>O<sub>4</sub>) as a catalyst or K<sub>2</sub>[Os<sup>VI</sup>O<sub>2</sub>(OH)<sub>4</sub>] as a precatalyst (Scheme 1a).<sup>1,2,11–20</sup> Intramolecular 1,2-aminohydroxylation of alkenes containing a nitrogen source in the molecule can also be accomplished using a similar catalytic system to obtain cyclic aminoalcohols with high regioselectivity (Scheme 1b).<sup>21–28</sup> Alkene 1,2-aminohydroxylation catalyzed by osmium-free metal compounds has also been examined using N-functionalized oxaziridine (Scheme 1c).<sup>29–34</sup> In this case, however, the resultant product is a mixture of the cis and trans isomers with respect to the -NR<sub>2</sub> and -OR groups, since the addition reaction proceeds in a stepwise manner.

## Scheme 1. Os<sup>VIII</sup>O<sub>4</sub>-Catalyzed cis-1,2-Aminohydroxylation (a, b) and Osmium-Free 1,2-Aminohydroxylation (c)



On the other hand, little attention has so far been focused on coordination compounds that consist of a metal center and

Received: May 14, 2015

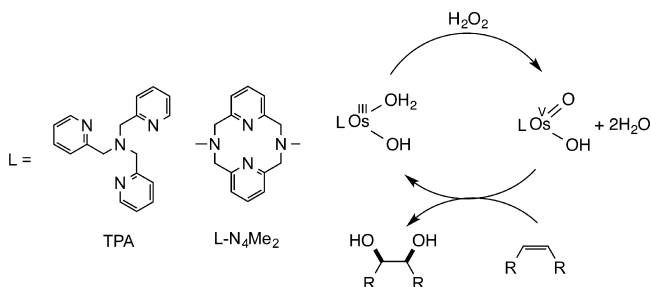
Published: June 30, 2015

organic ligands as the catalysts for 1,2-aminohydroxylation of alkenes. By changing the donor atoms, donor numbers, electron-donor ability, and geometry of the supporting ligands, one can finely tune reactivity of the catalysts. The reactivity of coordination compounds can also be controlled by altering the steric demand of the substituent of the ligands. Thus, development of a new class of coordination compounds that can catalyze *cis*-1,2-aminohydroxylation of alkenes will provide more efficient catalyst with higher reactivity and selectivity. Although cinchona alkaloids such as hydroquinine 1,4-phthalazinediyl diether ((DHQ)<sub>2</sub>PHAL) have been employed as a coligand of Os<sup>VIII</sup>O<sub>4</sub> for regio- and stereoselective aminohydroxylation of alkenes, the nature of the in situ generated compound is not clearly understood due to weak coordination ability of the alkaloid ligand.<sup>1,2,19</sup>

Our strategy for developing a new class of active oxidants is based on the synthesis of osmium coordination compounds that can adopt an oxidation state much lower than that of osmium(VIII). In addition, our system does not require addition of very toxic OsO<sub>4</sub> into the catalytic solution, thus eliminating any Os(VIII) species from the reaction system and making the reaction much safer to carry out.<sup>35,36</sup>

Recently, we developed an oxido-hydroxido-osmium(V) complex supported by tripodal tetradentate ligand tris(2-pyridylmethyl)amine (TPA) or macrocyclic tetradentate ligand *N,N'*-dimethyl-2,11-diaza[3.3](2,6)pyridinophane (L-N<sub>4</sub>Me<sub>2</sub>), which are capable of performing very efficient catalytic *cis*-dihydroxylation of various alkenes using H<sub>2</sub>O<sub>2</sub> as the terminal oxidant.<sup>37,38</sup> In this *cis*-1,2-dihydroxylation reaction, the Os-complex catalysts employ an Os(V)/Os(III) redox cycle, where the Os(V)(=O)(OH)(L) active species is regenerated by the reaction of Os(III)(OH)(OH<sub>2</sub>)(L) with H<sub>2</sub>O<sub>2</sub> (Scheme 2).<sup>37,38</sup>

### Scheme 2. *cis*-1,2-Dihydroxylation of Alkenes with H<sub>2</sub>O<sub>2</sub> Catalyzed by Os<sup>V</sup>(O)(OH)/ Os<sup>III</sup>(OH)(H<sub>2</sub>O) Centers



If an imido-hydroxido-osmium(V) Os(V)(=NR)(OH)(L) or an oxido-aminato-osmium(V) Os(V)(=O)(NHR)(L) oxidant can be generated from the precatalyst Os(III)(OH)(OH<sub>2</sub>)(L), using a nitrogen-containing oxidant, a new protocol for *cis*-1,2-aminohydroxylation of alkenes will be constructed, without producing any toxic Os<sup>VIII</sup> species. In this study, we succeeded in developing an efficient catalytic *cis*-1,2-aminohydroxylation of alkenes using *p*-tolSO<sub>2</sub>NCINa (chloramine-T) as the nitrogen-containing oxidant. Chloramine-T is a commercially available reagent and one of the oxidants employed most often in *cis*-1,2-aminohydroxylation catalyzed by OsO<sub>4</sub>.<sup>1,2,19</sup> We employ the Os<sup>III</sup>(OH)(OH<sub>2</sub>)(L) precursor complex supported by the rigid macrocyclic ligand (L = L-N<sub>4</sub>Me<sub>2</sub>) as a catalyst, [Os<sup>III</sup>(OH)(H<sub>2</sub>O)(L-N<sub>4</sub>Me<sub>2</sub>)](PF<sub>6</sub>)<sub>2</sub> (**1**; Figure 1). Density functional theory (DFT) calculation studies have suggested that an oxido-aminato-osmium(V) complex,

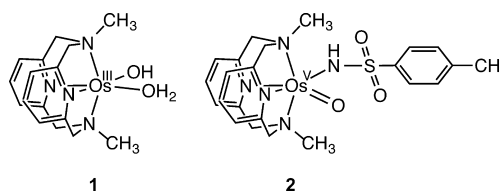


Figure 1. ChemDraw structures of complexes **1** and **2**.

[Os<sup>V</sup>(=O)(NHTs)(L-N<sub>4</sub>Me<sub>2</sub>)](ClO<sub>4</sub>)<sub>2</sub> (**2**; Figure 1), is the active oxidant in the stereoselective 1,2-aminohydroxylation reaction of alkenes.

## RESULTS AND DISCUSSION

### Catalytic *cis*-1,2-Aminohydroxylation of Cyclohexene.

Complex [Os<sup>III</sup>(OH)(H<sub>2</sub>O)(L-N<sub>4</sub>Me<sub>2</sub>)](PF<sub>6</sub>)<sub>2</sub> (**1**) was prepared according to the reported procedures.<sup>38</sup> At first, catalytic activity of **1** was examined in the reaction of cyclohexene with chloramine-T as a terminal oxidant (Table 1). Treatment of

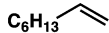
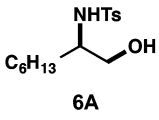
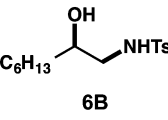
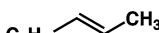
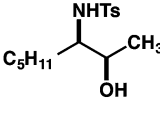
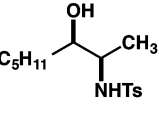
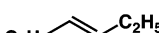
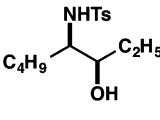
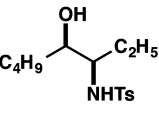
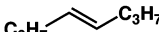
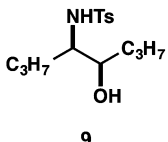

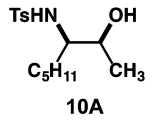
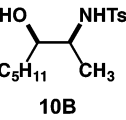
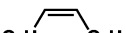
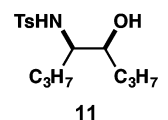
Table 1. Optimization of *cis*-1,2-Aminohydroxylation of Cyclohexene<sup>a</sup>

entry	cat (mol %)	temp (°C)	time (h)	yield (%) <sup>b</sup>		chemo-selectivity	ref
				5	diol		
1	1 (1.0)	30	5	46	7	6.6:1	<i>f</i>
2	1 (1.0)	50	5	42	10	4.2:1	<i>f</i>
3	1 (1.0)	70	5	37	8	4.6:1	<i>f</i>
4	1 (1.0)	30	10	56	10	5.6:1	<i>f</i>
5 <sup>c</sup>	1 (1.0)	30	5	51	11	4.5:1	<i>f</i>
6 <sup>d</sup>	1 (1.0)	30	5	53	10	5.5:1	<i>f</i>
7	OsO <sub>4</sub> (1.0)	60	12	59			12
8 <sup>e</sup>	OsO <sub>4</sub> (1.0)	25	6	65			12

<sup>a</sup>Reaction conditions: **1** (2.5 μmol) and substrate (250 μmol) were dissolved in H<sub>2</sub>O-*t*-BuOH (3 mL, 1:1 v/v). Chloramine-T (1 equiv) was added to the mixture, and the mixture was stirred under N<sub>2</sub>. <sup>b</sup>Determined by <sup>1</sup>H NMR. <sup>c</sup>With 3 equiv of chloramine-T. <sup>d</sup>With AgNO<sub>3</sub> (2.5 μmol). <sup>e</sup>With AgNO<sub>3</sub> (6.25 μmol). <sup>f</sup>This work.

chloramine-T (0.25 mmol) with cyclohexene (0.25 mmol) in a 1:1 mixture of H<sub>2</sub>O/*t*-BuOH (total 3.0 mL) in the presence of a catalytic amount of **1** (1 mol %) at 30 °C for 5 h gave *N*-(2-hydroxycyclohexyl)-4-methylbenzenesulfonamide (**5**) as a *cis*-1,2-aminohydroxylated product in a moderate yield (46%) together with *cis*-1,2-cyclohexanediol as a minor product (7%), where the chemoselectivity defined as a ratio of aminoalcohol/diol was 6.6 (entry 1). No other byproduct was obtained from the extracted organic layer (see Experimental Section). When the reaction was performed in H<sub>2</sub><sup>18</sup>O/*t*-BuOH (>98% H<sub>2</sub><sup>18</sup>O atom content), nearly quantitative incorporation of <sup>18</sup>O into **5** was observed (high-resolution mass spectrometry (HRMS (CI<sup>+</sup>): [M + H]<sup>+</sup> calculated 272.1164, found 272.1204), demonstrating that the oxygen source of the hydroxyl group was the solvent water. When the reaction was performed at higher temperature (entries 2 and 3; 50 and 70 °C, respectively), both the *cis*-1,2-aminoalcohol yield and the

Table 2. Catalytic *cis*-1,2-Aminohydroxylation of *n*-Octene ( $n = 1, 2, 3, 4$ )<sup>a</sup>

Entry	Substrate	Product		Regio- Selectivity (A : B) <sup>b</sup>	Yield (%) <sup>c</sup>
		A	B		
1				1 : 4.3	59
2				1 : 1.3	14
3				1 : 1	11
4				–	7
5				1 : 1.1	19
6				–	21

<sup>a</sup>Reaction conditions: **1** (2.5  $\mu$ mol), substrate (250  $\mu$ mol), chloramine-T (1 equiv) in H<sub>2</sub>O-*t*-BuOH (3 mL, 1:1 v/v) at 30 °C for 5 h under N<sub>2</sub>.  
<sup>b</sup>Determined by <sup>1</sup>H NMR. <sup>c</sup>Combined yield of the regioisomers.

chemoselectivity were slightly decreased. In the case of an OsO<sub>4</sub>-catalyzed system, on the other hand, the *cis*-1,2-aminoalcohol was produced in a 59% yield after the reaction of cyclohexene (5.0 mmol) with chloramine-T (5.0 mmol) in the presence of 1 mol % of OsO<sub>4</sub> at 60 °C for 12 h (entry 7).<sup>12</sup> Nearly the same yield was attained (56%), when the reaction time was elongated from 5 to 10 h in the present system (entry 4). These results indicate that toxic OsO<sub>4</sub> can be replaced with complex **1** as a catalyst for *cis*-1,2-aminohydroxylation of alkenes. Increase of the amount of chloramine-T (3 equiv) in the reaction solution did not improve the chemoselectivity (entry 5). Addition of silver nitrate (AgNO<sub>3</sub>) to the present catalytic system resulted in little effect on the product yield (entry 6), although AgNO<sub>3</sub> exhibited a beneficial effect in the OsO<sub>4</sub> system (65%, 25 °C, 6 h; entry 8).<sup>12</sup> On the basis of these results, the following catalytic conditions were employed in the *cis*-aminohydroxylation of other alkenes: amount of **1** = 1 mol %, alkene/reoxidant = 1:1, temperature = 30 °C, reaction time = 5 h.

**Catalytic *cis*-1,2-Aminohydroxylation of *n*-Octenes ( $n = 1, 2, 3, 4$ ).** Catalytic activity of **1** was then examined in *cis*-1,2-aminohydroxylation of a series of *n*-octenes (Table 2). Except for aminohydroxylation of *trans*- and *cis*-4-octenes (entries 4 and 6), two regioisomers, **A** and **B**, were formed. Among the products in Table 2, products **7A**, **8A**, **8B**, **10A**, and **11** were unknown compounds, whereas **6A**,<sup>39</sup> **7B**,<sup>40</sup> **9**,<sup>41</sup> and **10B**<sup>40</sup> have already been reported. The <sup>1</sup>H NMR and NOESY spectra of the new compounds, **7A**, **8A**, **8B**, **10A**, and **11**, are presented in Supporting Information Figures S1–S5. When 1-octene was employed, the aminoalcohols, **6A** and **6B**, were obtained in a 59% combined yield, where the product ratio of **6A** and **6B** was 1:4.3 (entry 1). In the case of aminohydroxylation of *trans*-2-, *trans*-3-, and *trans*-4-octenes, their *cis*-1,2-aminoalcohols with a threo configuration were selectively obtained (**7A**, **7B**, **8A**, **8B**, and **9**, entries 2, 3, and 4). The product yield drastically decreased in going from 1-octene to *trans*-2-octene (59 → 14%) and slightly decreased in going from *trans*-2-octene to *trans*-3-octene and to *trans*-4-octene (14 → 11 → 7%). The results clearly indicate that less-hindered

Table 3. Catalytic *cis*-1,2-Aminohydroxylation of Electron-Deficient Alkenes<sup>a</sup>

Entry	Substrate	Product	Regio-Selectivity (A : B) <sup>b</sup>	Yield (%) <sup>c</sup>
1			–	25 (68)
2 <sup>d</sup>			–	37 (92)
3 <sup>d</sup>			–	17 (46)
4			2.3 : 1	28 (88)
5			1 : 2.0	65
6			1 : 4.5	26
7			1.6 : 1	71

<sup>a</sup>Reaction conditions: **1** (2.5 μmol), substrate (250 μmol), chloramine-T (1 equiv) in H<sub>2</sub>O–*t*-BuOH (3 mL, 1:1 v/v) at 30 °C for 5 h under N<sub>2</sub>.  
<sup>b</sup>Determined by <sup>1</sup>H NMR. <sup>c</sup>Combined yield of the regioisomers (at 100% alkene conversion); parentheses indicate conversion yields. <sup>d</sup>Catalytic reaction was performed in a suspension of the substrate due to the poor solubility.

double bond is more susceptible for the aminohydroxylation. Furthermore, the regioselectivity in 1-octene aminohydroxylation was meaningfully higher than those in *trans*-2- and *trans*-3-octenes, which indicates that the hindered tosylamino functional group favored less-hindered carbon atom to avoid steric repulsion with more-hindered C1 carbon atom of the double bond. However, when *cis*-2- and *cis*-4-octenes were employed as substrates, their *cis*-1,2-aminoalcohols having an erythro form were selectively obtained in 19 and 21% yields, respectively (**10A**, **10B**, and **11**, entries 5 and 6). The higher reactivity of the *cis*-octenes when compared with the corresponding *trans*-octenes reveals that the present *cis*-1,2-aminohydroxylation favors less-hindered C=C double bonds as mentioned above. Similar tendency was observed in the *cis*-1,2-dihydroxylation of a series of octenes with H<sub>2</sub>O<sub>2</sub> catalyzed by complex **1**.<sup>39</sup> The selective formation of the threo and erythro products from *trans*- and *cis*-octenes clearly demonstrates that the present *cis*-1,2-aminohydroxylation proceeded exclusively via syn addition to the C=C double bond.

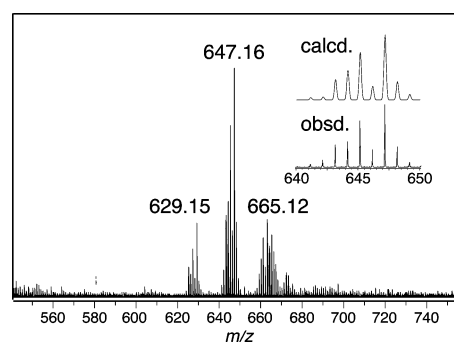
**Catalytic *cis*-1,2-Aminohydroxylation of Electron-Deficient Alkenes.** Electron-deficient alkenes were generally converted into the corresponding *cis*-1,2-aminoalcohols with modest to high yields (Table 3). The yields of **12**, **13**, and **14** obtained from the symmetric alkenes having an internal C=C double bond were higher than those of **9** and **11** obtained from *trans*- and *cis*-4-octenes (entries 1, 2, and 3 in Table 3 vs entries of 4 and 6 in Table 2), where entries 2 and 3 were performed under heterogeneous conditions due to low solubility of the substrates. The yield of **13** obtained from *trans*-stilbene was higher than that of **14** obtained from the *cis* isomer, which may be ascribed to the relatively higher solubility of *trans*-stilbene. With respect to the aminohydroxylation of 4-octenes, the *cis* isomer was converted to the aminoalcohol more effectively than the *trans* isomer. The unsymmetric substrates were also converted to their aminoalcohols in modest to high yields. When methyl cinnamate was employed, the tosylamino group favored more electron-deficient carbon atom (entry 4), where the regioselectivity of **15A/15B** was 2.3:1. In the aminohydroxylation of styrene (entry 5), the terminal carbon atom

was predominantly aminated to give **16A** and **16B** in a 1:2.0 ratio. Introduction of a methyl group on the  $\alpha$ -position of styrene increased the regioselectivity from 1:2.0 to 1:4.5 (**17A** and **17B**, entry 6). On the other hand, by introduction of a methyl group to the  $\beta$ -position of styrene, the more electron-deficient  $\alpha$ -carbon atom is predominantly aminated to give the inversed regioselectivity 1.6:1 (**18A** and **18B**, entry 7). The regioselectivity in entry 4 was comparable to that obtained by the OsO<sub>4</sub> catalytic system (2:1), whereas those in entries 5 and 7 were higher than those in the OsO<sub>4</sub>-catalyzed reactions (1:1.5 and 1:1).<sup>12</sup>

**Mechanistic Aspects.** In the aminohydroxylation of alkenes catalyzed by OsO<sub>4</sub>, the active oxidant has been identified as trioxido–imido–osmium(VIII), Os<sup>VIII</sup>O<sub>3</sub>(NR).<sup>42</sup> Recently, we demonstrated that an oxido–hydroxido–osmium(V) complex, Os<sup>V</sup>(O)(OH)(L), supported by tetradentate ligands L (L = L-N<sub>4</sub>Me<sub>2</sub> and TPA), worked as the new active oxidant for cis-1,2-dihydroxylation of alkenes (Scheme 2).<sup>37,38</sup> The active oxidants were generated by oxidation of their hydroxido–aquo–osmium(III) precursors Os<sup>III</sup>(OH)(OH<sub>2</sub>)(L) with hydrogen peroxide.<sup>37,38</sup> To obtain insights into the catalytic cycle of the present cis-1,2-aminohydroxylation, we tried to characterize the active oxidant by some spectroscopic methods. Furthermore, the structure and the reaction pathways were examined by DFT calculations.

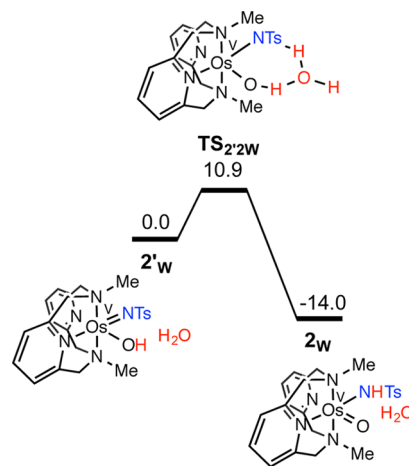
First, the catalytic aminohydroxylation of methyl cinnamate was performed in the presence of an equal amount of chiral ligands such as (DHQD)<sub>2</sub>AQN, (DHQD)<sub>2</sub>AQN, or (DHQD)<sub>2</sub>PHAL together with complex **1**. In this case, a racemic mixture of the aminoalcohol products **15A** and **15B** was obtained,<sup>43</sup> indicating that neither free Os<sup>VIII</sup>O<sub>4</sub> nor Os<sup>VIII</sup>O<sub>3</sub>(NTs) was generated during our present system. If such Os(VIII) species were generated during the reaction of **1** with chloramine-T, combination of the Os(VIII) species and the chiral ligand might give chiral aminoalcohols with a high enantioselectivity as reported by Sharpless et al.<sup>16</sup> Thus, an osmium(V) species may be formed as the active species as in the case of our previous cis-dihydroxylation reaction.<sup>37,38</sup> Addition of 1 equiv of chloramine-T to a solution of **1** at 0 °C resulted in a color change from orange to brown. After keeping the resultant solution in a refrigerator at ca. 2 °C, purple-brown powder was precipitated, the IR spectrum of which showed the presence of tosyl (Ts) group.<sup>44</sup> Moreover, the UV–vis spectrum of the purple-brown product in acetone was quite similar to that of the oxido–hydroxido–osmium(V) complex previously reported,<sup>38</sup> suggesting formation of a similar type of osmium(V) species (see Experimental Section). The CSI-mass spectrum of the product dissolved in H<sub>2</sub>O is shown in Figure 2. The spectrum showed a peak cluster at  $m/z$  = 647.16, the isotope distribution pattern of which was consistent with the chemical formula of {Os + (NTs) + (OH) + (L-N<sub>4</sub>Me<sub>2</sub>) + H}<sup>+</sup> or {Os + (NHTs) + (O) + (L-N<sub>4</sub>Me<sub>2</sub>) + H}<sup>+</sup>. The effective magnetic moment of the product complex in acetone determined by Evans method was  $\mu = 1.0 \mu_B$ ,<sup>45</sup> indicating that the osmium center has a doublet ground state ( $S = 1/2$ ) with a (d<sub>xy</sub>)<sup>2</sup>(d<sub>yz</sub>)<sup>1</sup>(d<sub>zx</sub>)<sup>0</sup> configuration.<sup>46</sup> The electron configuration is typical as a six-coordinate oxido-d<sup>3</sup> metal complex.<sup>47</sup>

A possible reactive species could be an oxido–tosylaminate–osmium(V), [Os<sup>V</sup>(=O)(–NHTs)(L-N<sub>4</sub>Me<sub>2</sub>)]<sup>2+</sup> (**2**), or an imido–hydroxido–osmium(V), [Os<sup>V</sup>(–OH)(=NTs)(L-N<sub>4</sub>Me<sub>2</sub>)]<sup>2+</sup> (**2'**). The DFT calculation study indicated that the former complex **2** is more stable than the latter complex **2'**



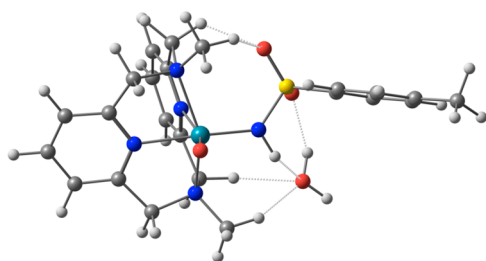
**Figure 2.** Positive CSI-mass spectrum of **2** obtained from a reaction of **1** with chloramine-T. Temperature = 0 °C. Solvent = H<sub>2</sub>O.

by 6.2 kcal/mol. The calculations also suggested that the Os(V) center of **2** has a doublet ground state with a (d<sub>xy</sub>)<sup>2</sup>(d<sub>yz</sub>)<sup>1</sup>(d<sub>zx</sub>)<sup>0</sup> configuration, which is consistent with the experimental result mentioned above (Evans method). Complex **2** may be formed from the initially generated **2'** by intramolecular proton transfer from the hydroxide ligand to the imide ligand. The calculations suggested that the free energy of activation for the conversion of **2'** to **2** by direct proton transfer from the Os–OH moiety to the Os–NTs group is 39.4 kcal mol<sup>–1</sup>, which is inaccessible in the present experimental conditions. However, it was found that a water molecule significantly accelerates the conversion with a low activation barrier of 10.9 kcal mol<sup>–1</sup> as indicated in Figure 3. The proton transfer occurs through a water molecule



**Figure 3.** Free energy profile for the water-assisted isomerization reaction. Units are in kilocalories per mole.

via the transition state of TS<sub>2'2w</sub> to yield water-incorporated oxido–tosylaminate–osmium(V) complex **2<sub>w</sub>**, which is energetically more preferred than the water-incorporated imido–hydroxido–osmium(V) complex **2'<sub>w</sub>** by 14.0 kcal mol<sup>–1</sup>. Association of the additional water molecule was supported experimentally by the appearance of a peak cluster at  $m/z$  = 665.12, which is 18 mass units larger than the parent peak at 647.16. A DFT-optimized geometry of the key intermediate **2<sub>w</sub>** is given in Figure 4. The Os–NHTs and Os=O bond distances in **2<sub>w</sub>** are 1.922 and 1.724 Å, respectively, which are close to the Os–OH and Os=O distances in the crystal structure of the oxido–hydroxido–osmium(V) complex [Os<sup>V</sup>(O)(OH)(L-N<sub>4</sub>Me<sub>2</sub>)](PF<sub>6</sub>)<sub>2</sub>, where the corresponding distances are, respectively, 1.921(4) and 1.753(5) Å.<sup>38</sup> Mulliken charge analysis suggested that the oxygen atom of the oxide



**Figure 4.** DFT-calculated three-dimensional structure of **2<sub>w</sub>**; green: osmium, blue: nitrogen, red: oxygen, gray: carbon, yellow: sulfur, white: hydrogen. Mulliken charges; Osmium 1.00, N(-HTs) -0.04, O (oxide) -0.41. Os-O (oxide): 1.724 Å, Os-N(-HTs) 1.922 Å. Selected atomic distances are in angstroms.

group (-0.41) of **2<sub>w</sub>** is more electronegative than the nitrogen atom of the NHTs group (-0.04). Spin densities of the Os, O, and N atoms are +0.62, +0.42, and -0.06, respectively, which clearly indicates that the singly occupied molecular orbital of **2<sub>w</sub>** consists of  $d\pi-p\pi$  antibonding interactions between the Os and oxide oxygen atoms.

*cis*-1,2-Aminohydroxylation of a series of *para*-substituted styrenes ( $p$ -X-C<sub>6</sub>H<sub>4</sub>CH=CH<sub>2</sub>; X = OMe, Me, H, Cl, CF<sub>3</sub>) with 1 equiv of chloramine-T was also examined in the presence of 1 mol % of complex **1**. The regioselectivity of the products and the combined yield of the regioisomers are summarized in Table 4. Among the five entries, the combined

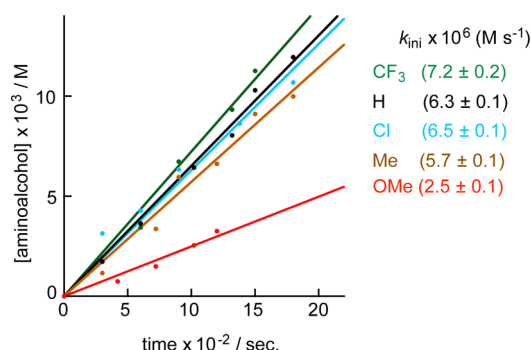
**Table 4.** Catalytic *cis*-1,2-Aminohydroxylation of *p*-Substituted Styrenes<sup>a</sup>

Entry	<i>p</i> -Substituent	Regio-selectivity <sup>b</sup>		Yield (%) <sup>c</sup>
		NHTs Ph	OH Ph	
1	OMe	1 ( <b>19A</b> )	2.2 ( <b>19B</b> )	36
2	Me	1 ( <b>20A</b> )	1.4 ( <b>20B</b> )	57
3	H	1 ( <b>21A</b> )	1.8 ( <b>21B</b> )	65
4	Cl	1 ( <b>22A</b> )	2.1 ( <b>22B</b> )	66
5	CF <sub>3</sub>	1 ( <b>23A</b> )	1.9 ( <b>23B</b> )	71

<sup>a</sup>Reaction conditions: **1** (2.5 μmol), substrate (250 μmol), chloramine-T (1 equiv) in H<sub>2</sub>O-*t*-BuOH (3 mL, 1:1 v/v) at 30 °C for 5 h under N<sub>2</sub>. <sup>b</sup>Determined by <sup>1</sup>H NMR. <sup>c</sup>Combined yield of the regioisomers.

yield for the aminohydroxylation of *p*-OMe-C<sub>6</sub>H<sub>4</sub>CH=CH<sub>2</sub> was significantly low (entry 1, 36%). With respect to the other substrates (entries 2–5), the combined yield slightly increased as the *para*-substituent became more electron-withdrawing from X = Me (57%) to X = CF<sub>3</sub> (71%) though the yields of the aminoalcohols in entries 3 (X = H, 65%) and 4 (X = Cl, 66%) were nearly equal. No significant difference was found in the regioselectivity of the amino alcohols in all reactions, suggesting that an electronic effect of the *para* substituents hardly controls the regioselectivity.

Then, the formation of aminoalcohols at the initial stage of the reaction was monitored by high-performance liquid chromatography (HPLC; see Experimental Section). Figure 5 shows the plots of the product yields (M) versus the reaction time. The initial rate ( $k_{\text{ini}}$ , M s<sup>-1</sup>) for the formation of aminoalcohols with X = OMe was significantly smaller than those of the other aminoalcohols. However, the initial rates of

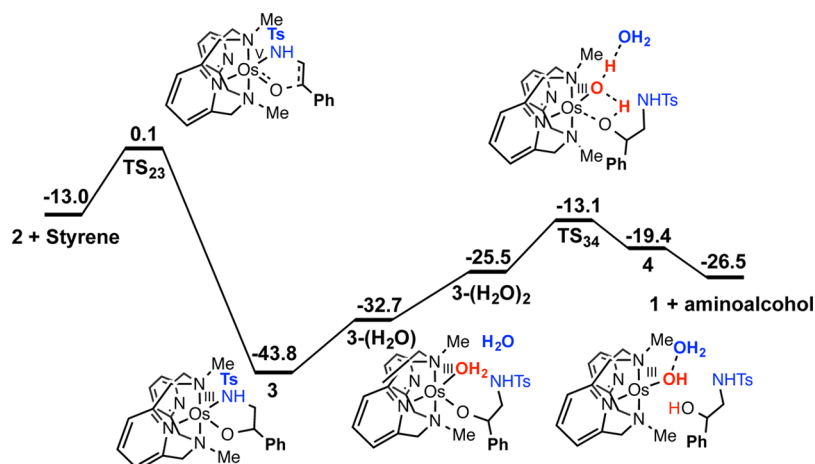


**Figure 5.** Time course of the product yield for the *cis*-1,2-aminohydroxylation of a series of *para*-substituted styrenes ( $p$ -X-C<sub>6</sub>H<sub>4</sub>CH=CH<sub>2</sub>; X = OMe, Me, H, Cl, CF<sub>3</sub>).

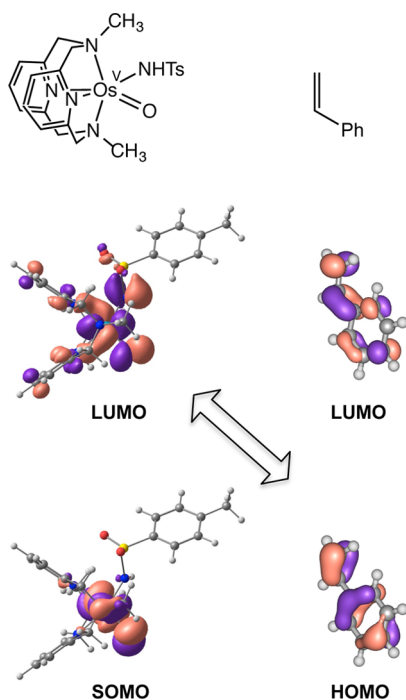
formation of the other amino alcohols were relatively close to each other even though there is a tendency that the rate slightly increased as the X substituent became more electron-negative; X = Me ((5.7 ± 0.1) × 10<sup>-6</sup> M s<sup>-1</sup>), H ((6.3 ± 0.1) × 10<sup>-6</sup> M s<sup>-1</sup>), Cl ((6.5 ± 0.1) × 10<sup>-6</sup> M s<sup>-1</sup>), CF<sub>3</sub> (7.2 ± 0.2) × 10<sup>-6</sup> M s<sup>-1</sup>). This trend was consistent with the substituent effects found in their product yields (Table 4).

Oxido-tosylamino-osmium(V) complex **2** generated from **1** and chloramine-T reacted with cyclohexene in a H<sub>2</sub>O-*t*-BuOH mixed solvent to yield its aminoalcohol product (see Experimental Section). Having established that **2** is an active species in the reaction, further DFT calculations were performed to gain better understanding of the mechanism of the aminohydroxylation. Since two regioisomers were produced from the aminohydroxylation of an unsymmetrical alkene, we examined the reaction pathways of styrene as a representative substrate to explore the selectivity of the reaction. A calculated free energy profile for the reaction pathway leading to the formation of the major regioisomer is shown in Figure 6. The optimized structures of the intermediates and transition states involved in the pathway are provided in the Supporting Information (Figure S6). The first step of the reaction involves a [3 + 2] cycloaddition between **2** and styrene via a concerted transition state **TS<sub>23</sub>**. The concerted cycloaddition is initiated by the nucleophilic attack of the highest occupied molecular orbital of styrene to the lowest unoccupied molecular orbital of **2**. This step requires an activation barrier of 13.1 kcal mol<sup>-1</sup>. In Figure 7 the representative frontier molecular orbitals (MOs) are in phase in the reaction site, which is consistent with the concerted reaction of the [3 + 2] cycloaddition. The resultant **TS<sub>23</sub>** exhibits the C1 (styrene)⋯N (tosylamino) distance of 2.133 Å and C2 (styrene)⋯O (oxide) distance of 2.314 Å. Then, the five-membered osmium 1-tosylamino-2-phenylethanol intermediate **3** is formed from **TS<sub>23</sub>**. Formation of **3** is exergonic by 30.8 kcal mol<sup>-1</sup> and causes a decrease in the positive charge of Os from +0.60 to +0.25, which corresponds to the reduction of the osmium center from +V to +III. In **3**, the C1 (styrene)⋯N and C2 (styrene)⋯O (oxide) distances are, respectively, found to be 1.490 and 1.422 Å.

Next, the elimination process comprises hydrolysis of **3** with two water molecules. The first water molecule replaces the weakly coordinated nitrogen atom of the tosylamino group and binds to the osmium center to yield **3**-(H<sub>2</sub>O), and then **3**-(H<sub>2</sub>O) associates with a second water molecule, resulting in the formation of **3**-(H<sub>2</sub>O)<sub>2</sub>. The addition of first and second water molecule to **3** is found to be endergonic by 11.1 and 7.2 kcal mol<sup>-1</sup>, respectively. Next step is the proton transfer from the



**Figure 6.** Computed reaction mechanism for the aminohydroxylation of styrene. Relative free energies with respect to **2'** are reported in units of kilocalories per mole.



**Figure 7.** Representative frontier MO interactions in the [3 + 2]-type concerted reaction for aminohydroxylation of styrene with **2**.

first water molecule to the alkoxide oxygen atom through a four-membered transition state  $\text{TS}_{34}$ . This step is endergonic by 6.1 kcal/mol with an activation barrier of 12.4 kcal mol<sup>-1</sup>. In  $\text{TS}_{34}$ , the Os–O<sub>alkoxide</sub> bond is elongated from 1.946 to 2.076 Å. As a result of this transition state, the product aminoalcohol is generated on osmium center **4**, and the successive coordination of the second water molecule to the five-coordinate osmium atom regenerates the starting hydroxido–aquo–osmium(III) complex **1**. Overall, the reaction is exergonic by –26.5 kcal mol<sup>-1</sup>.

A computed Gibbs free energy diagram for the reaction leading to the formation of the minor regioisomer (C<sub>6</sub>H<sub>5</sub>CH(NHTs)CH<sub>2</sub>(OH)) is given in the Supporting Information (Figure S7). The optimized structures of the intermediates and transition states involved in the pathway are provided in Supporting Information, Figure S8. Comparison of the reaction

pathway of the major and minor regioisomers indicates that the [3 + 2]-type concerted transition state for the minor regioisomer is slightly lower in energy than that of major isomer. However, the intermediates and transition state for the rest of the reaction are lying higher in energy. The cycloaddition product, denoted as **3'**, is 6.3 kcal mol<sup>-1</sup> less stable than **3**. Similarly, the other intermediates as well as transition state, denoted as **3'-(H<sub>2</sub>O)**, **3'-(H<sub>2</sub>O)<sub>2</sub>**,  $\text{TS}_{3'4'}$ , **4'**, and the final product are higher in energy by 7.6, 8.1, 5.3, 7.3, and 3.1 kcal mol<sup>-1</sup>, respectively, when compared with the corresponding structures for the major regioisomer. The relative higher energies of these intermediates are probably due to the restriction of free movement of phenyl ring and the steric effect caused by tosylamino group, whereas such an effect is not pronounced in the initial reactant complex and the cycloaddition transition state. Though the initial step of the reaction favors a minor regioisomer, the following steps disfavor the reaction to occur easily due to the steric constraints. This suggests that the orientation of substrate with less sterically hindered group close to the tosylamino group leads to the formation of major isomer. It is also evident in the case of  $\alpha$ -methylstyrene (entry 6 of Table 3), where the orientation of carbon atom having Me and Ph groups toward the oxido group of osmium center leads to the major regioisomer.

It is worth noting that introduction of a methylcarboxylate or a methyl group at the  $\beta$ -position of styrene reversed the regioselectivity (entries 4 and 7 in Table 3). To examine the reversal of regioselectivity, we also extended the DFT study to the reaction pathways of methyl cinnamate (entry 4 in Table 3). In this case, the rate-determining [3 + 2]-type concerted transition state is destabilized by 5.3 kcal/mol when the carbon atom bearing –COOMe group is associated with the tosylamino group compared to the orientation for major isomer. Thus, sterically less-affected orientation in which the carbon atom having Ph group toward the tosylamino group leads to the formation of major regioisomer. All these details are given in the Supporting Information (Figures S9–S11).

Thus, on the basis of the  $k_{\text{ini}}$  values in the catalytic aminohydroxylation of styrenes (Figure 5), the following are suggested. In the formation of the four aminoalcohols with X = Me, H, Cl, and CF<sub>3</sub>, the electron-donating or electron-withdrawing nature of the X substituents affects oppositely

the  $k_d$  and  $k_a$  processes, respectively, where the  $k_a$  process consists of association of the active oxidant **2**, and the styrenes and  $k_d$  process is a dissociation path of the corresponding amino alcohols formed from the osmium center of **3**. The opposite effects may cancel out the electronic effects of the X groups on the formation rate at the initial stage to give the nearly same  $k_{ini}$  values for the four styrenes. However, the  $k_d$  process may dominate the catalytic reaction for formation of styrene with X = OMe since the electron-donating property of the OMe group stabilizes the formed aminoalcoholate–osmium(III) intermediate.

## CONCLUSION

We herein presented a new protocol that employs the hydroxido–aquo–osmium(III) complex  $[\text{Os}^{\text{III}}(\text{OH})(\text{H}_2\text{O})(\text{L}-\text{N}_4\text{Me}_2)]^{2+}$  (**1**) supported by a tetradentate macrocyclic amine ligand as a catalyst for cis-aminohydroxylation of alkenes with chloramine-T as an oxidant and a nitrogen donor. Various types of alkenes from electron-rich alkenes to electron-deficient alkenes are converted syn-selectively to their cis-1,2-aminoalcohols (18 examples). Two regioisomers are produced from the aminohydroxylation of unsymmetrical alkenes, and their selectivity is thermodynamically controlled. A combination of spectroscopic methods including cold mass measurements and DFT calculations for the reaction of **1** with chloramine-T have indicated that the osmium(III) complex is oxidized with chloramine-T to give  $[\text{Os}^{\text{V}}(-\text{OH})(=\text{NTs})(\text{L})]^{2+}$  (**2'**), which immediately isomerizes to  $[\text{Os}^{\text{V}}(=\text{O})(-\text{NHTs})(\text{L})]^{2+}$  (**2**) via the water-assisted intramolecular proton transfer. DFT calculations have further suggested that **2** reacts with alkene via concerted [3 + 2] cycloaddition and that the resultant five-membered aminoalkoxide osmium(III) intermediate (**3**) is hydrolyzed to yield the product and starting catalyst **1**. Because the oxido–alkylamino–osmium(V) species **2** in the present protocol is a novel active oxidant in direct cis-aminohydroxylation of alkenes and the reactivity can be controlled by the supporting ligand, the present protocol can open development of alternative methods for cis-aminohydroxylation of alkenes.

## EXPERIMENTAL SECTION

**General.** All reagents and solvents were used as received unless otherwise noted. The compound  $[\text{Os}^{\text{III}}(\text{OH})(\text{H}_2\text{O})(\text{L}-\text{N}_4\text{Me}_2)](\text{PF}_6)_2$  (**1**) was prepared by following the reported procedure.<sup>38</sup> <sup>1</sup>H NMR spectra were recorded at 400 MHz on a JEOL-ECS400 and at 600 MHz on a BRUKER. Cold electrospray ionization mass spectra (ESI-MS) measurements were performed on a BRUKER cryospray microOTOFII.

$[\text{Os}^{\text{V}}(\text{O})(\text{NHTs})(\text{L}-\text{N}_4\text{Me}_2)]\text{PF}_6)_2$  (**2**). Complex **1** (16.0 mg, 20.0  $\mu\text{mol}$ ) was dissolved into water (1 mL) at 40 °C. Chloramine-T (6.0 mg, 20.0  $\mu\text{mol}$ ) dissolved in water (0.25 mL) was added dropwise to the solution of **1**. Color of the solution immediately changed from orange to brown.  $\text{NH}_4\text{PF}_6$  (7.0 mg, 40.0  $\mu\text{mol}$ ) dissolved in water (0.25 mL) was added to the solution, and the resultant solution was kept standing in refrigerator overnight. Purple-brown powder precipitated from the solution, which was collected by filtration and dried in vacuo. Yield 7.0 mg (37%). The powder was highly hygroscopic. Anal. Calcd for  $2 \cdot 4.5\text{H}_2\text{O}$  ( $\text{C}_{23}\text{H}_{37}\text{N}_5\text{O}_{7.5}\text{F}_{12}\text{SP}_2\text{Os}$ ): C, 27.20; H, 3.67; N, 6.89%. Found: C, 26.89; H, 3.48; N, 7.34%. FT-IR (KBr): 1690 (w), 1638 (w), 1616 (m), 1584 (w), 1487 (w), 1468 (m), 1455 (m), 1405 (w), 1332 (w), 1166 (w), 1128 (w), 999 (w), 974 (w), 921 (w), 837 (vs), 801 (m), 761 (w), 740 (w), 559 (s). UV–vis ( $\text{H}_2\text{O}$ ):  $\lambda_{\text{max}}$  = 251 nm ( $\epsilon$  = 7590  $\text{M}^{-1}\text{cm}^{-1}$ ), 259 (6580), 274 (4070), 343 (2880), 462 (1920), 529 (1760). The UV–vis spectrum was measured at once after dissolution of the powder in  $\text{H}_2\text{O}$ .

**Standard Procedure for Catalytic cis-1,2-Aminohydroxylation of Alkenes.** A  $\text{H}_2\text{O}$ –*t*-BuOH (1:1 v/v, 3.0 mL) solution of **1** (1.98 mg, 2.5  $\mu\text{mol}$ ) was degassed by bubbling  $\text{N}_2$  for 30 min. The alkene (250  $\mu\text{mol}$ ) and chloramine-T (TsNCINa) (70.4 mg, 250  $\mu\text{mol}$ ) in 1 mL of  $\text{H}_2\text{O}$ –*t*-BuOH (1:1 v/v) were added to the solution, and the resulting mixture was stirred for 5 h. After the catalytic reaction, the organic products were extracted with 15 mL portions of diethyl ether five times, and the combined organic layer was concentrated by a rotary evaporator. The products were identified by <sup>1</sup>H NMR and NOESY spectra and HRMS. Yields of the products were determined from the <sup>1</sup>H NMR spectra, where an integral ratio of the protons was compared with the integration ratio of the protons ( $\text{Cl}-\text{CH}-\times 2$ ) of 1,1,2,2-tetrachloroethane added as an internal standard (250  $\mu\text{mol}$ ). The catalytic experiments were performed at least three times for each entry.

**Aminohydroxylation of Cyclohexene with **2**.** **2** was formed by a stoichiometric reaction of **1** (5.0 mg, 6.4  $\mu\text{mol}$ ) with chloramine-T (1.8 mg, 6.5  $\mu\text{mol}$ ) in a  $\text{H}_2\text{O}$ –*t*-BuOH mixed solvent (1.5 mL) at room temperature. Formation of **2** was confirmed by the UV–vis spectrum. Then, 0.5 mL of a  $\text{H}_2\text{O}$ –*t*-BuOH solution of cyclohexene (16.7  $\mu\text{L}$ , 64.0  $\mu\text{mol}$ ) was added to the solution of **2** at room temperature. The resulting solution was stirred for 5 h. The organic product was extracted with 15 mL portions of diethyl ether three times. The combined organic layer was dried over  $\text{Na}_2\text{SO}_4$  and  $\text{Na}_2\text{SO}_4$  was removed by filtration. The filtrate was removed by a rotary evaporator to give a brown solid. The yield of **5** was determined to be 15% from the <sup>1</sup>H NMR spectrum using 1,1,2,2-tetrachloroethane as an internal standard.

**Time Course Analysis of cis-1,2-Aminohydroxylation of Styrenes.** A  $\text{H}_2\text{O}$ –*t*-BuOH (1:1 v/v, 3.0 mL) solution containing complex **1** (1.98 mg, 2.5  $\mu\text{mol}$ ) was degassed by bubbling  $\text{N}_2$  for 30 min. The substrate (250  $\mu\text{mol}$ ) and chloramine-T (70.4 mg, 250  $\mu\text{mol}$ ) in 1 mL of  $\text{H}_2\text{O}$ –*t*-BuOH (1:1 v/v) was introduced into the solution. The time course of the initial stage of the reaction (30 min) was followed by an HPLC system of a Shimadzu LD10AV series equipped with a reverse-phase column (Nacal tesque, COSMOCIL, SC18-AR-II). A portion of the reaction solution (10  $\mu\text{L}$ ) was taken by a microsyringe every 5 min and diluted with 500  $\mu\text{L}$  of acetonitrile containing anisole as an internal standard (1.0 mM), which was used for the HPLC analysis. After 5 h, the final reaction solution was worked up and analyzed as stated above.

**Characterization Data.** The <sup>1</sup>H NMR spectra and HRMS (FAB<sup>−</sup>) of **5**, **6A**, **6B**, **7B**, **9**, **10B**, **12**, **13**, **14**, **15A**, **15B**, **16A**, **16B**, **17A**, **17B**, **18A**, **18B**, **19B**, **20B**, **21A**, **21B**, **22B**, and **23B** were identical with those of the compounds in literature.<sup>12,19,39–41,48,49</sup>

*threo*-2-Hydroxy-3-amino-*N*-[(4-methylphenyl)sulfonyl]octane (**7A**). <sup>1</sup>H NMR (400 MHz,  $\text{CDCl}_3/\text{TMS}$ ) = 7.75 (d,  $J$  = 8.0 Hz, 2H), 7.29 (d,  $J$  = 8.0 Hz, 2H), 4.56 (d,  $J$  = 6.8 Hz, 1H), 3.76 (m, 1H), 3.07 (m, 1H), 2.42 (s, 3H) 1.80 (d,  $J$  = 4.8 Hz), 1.15–1.30 (m, 2H), 0.95–1.15 (m, 4H), 1.11 (d,  $J$  = 6.4 Hz, 3H), 0.78 (t,  $J$  = 7.2 Hz, 3H) ppm; HRMS (FAB<sup>−</sup>)  $[\text{M}-\text{H}]^+$  calculated for  $\text{C}_{15}\text{H}_{24}\text{NO}_3\text{S}$  298.1477, found 298.1480. The NOE spectrum is given in Figure S2 of the Supporting Information.

*threo*-3-Hydroxy-4-amino-*N*-[(4-methylphenyl)sulfonyl]octane (**8A**). <sup>1</sup>H NMR (400 MHz,  $\text{CDCl}_3/\text{TMS}$ ) = 7.76 (d,  $J$  = 8.4 Hz, 2H), 7.29 (d,  $J$  = 8.4 Hz, 2H), 4.61 (d,  $J$  = 8.8 Hz, 1H), 3.55 (m, 1H), 3.09 (m, 1H), 2.42 (s, 3H) 1.53 (d,  $J$  = 4.8 Hz, 1H), 1.1–1.4 (m, 6H), 0.7–0.9 (br, 2H), 0.84 (t,  $J$  = 7.4 Hz, 3H), 0.77 (t, 7.2 Hz, 3H) ppm; HRMS (FAB<sup>−</sup>)  $[\text{M}-\text{H}]^+$  calculated for  $\text{C}_{15}\text{H}_{24}\text{NO}_3\text{S}$  298.1477, found 298.1479. The NOE spectrum is given in Figure S3 of the Supporting Information.

*threo*-3-Amino-4-hydroxy-*N*-[(4-methylphenyl)sulfonyl]octane (**8B**). <sup>1</sup>H NMR (400 MHz,  $\text{CDCl}_3/\text{TMS}$ ) = 7.76 (d,  $J$  = 8.0 Hz, 2H), 7.29 (d,  $J$  = 8.0 Hz, 2H), 4.54 (d,  $J$  = 9.2 Hz, 1H), 3.47 (m, 1H), 3.18 (m, 1H), 2.43 (s, 3H), 1.58 (d,  $J$  = 4.0 Hz, 1H), 1.1–1.5 (m, 8H), 0.88 (t, 7.6 Hz, 3H), 0.76 (t, 7.2 Hz, 3H) ppm. HRMS (FAB<sup>−</sup>)  $[\text{M}-\text{H}]^+$  calculated for  $\text{C}_{15}\text{H}_{24}\text{NO}_3\text{S}$  298.1477, found 298.1479. The NOE spectrum is given in Figure S4 of the Supporting Information.

*erythro*-2-Hydroxy-3-amino-*N*-[(4-methylphenyl)sulfonyl]octane (**10A**). <sup>1</sup>H NMR (400 MHz,  $\text{CDCl}_3/\text{TMS}$ ) = 7.77 (d,  $J$  = 8.4 Hz, 2H),



7.31 (d,  $J = 8.4$  Hz, 2H), 4.43 (d,  $J = 8.0$  Hz, 1H), 3.76 (m, 1H), 3.19 (m, 1H), 2.43 (s, 3H) 2.13 (d,  $J = 6.8$  Hz, 1H), 1.15–1.40 (m, 4H), 1.10 (d,  $J = 6.4$  Hz, 3H), 0.95–1.10 (m, 2H), 0.80–0.95 (m, 2H), 0.76 (t,  $J = 6.8$  Hz, 3H) ppm; HRMS (FAB<sup>-</sup>) [M-H]<sup>+</sup> calculated for C<sub>15</sub>H<sub>24</sub>NO<sub>3</sub>S 298.1477, found 298.1478. The NOE spectrum is given in Figure S5 of the Supporting Information.

**erythro-4-Hydroxy-5-amino-N-[(4-methylphenyl)sulfonyl]octane (11).** <sup>1</sup>H NMR (400 MHz, CDCl<sub>3</sub>/TMS) = 7.76 (d,  $J = 8.0$  Hz, 2H), 7.30 (d,  $J = 8.0$  Hz, 2H), 4.54 (d,  $J = 8.8$  Hz, 1H), 3.48 (m, 1H), 3.20 (m, 1H), 2.42 (s, 3H), 1.79 (d,  $J = 6.8$  Hz, 1H), 1.10–1.45 (m, 8H), 0.88 (t,  $J = 6.8$  Hz, 3H), 0.74 (t,  $J = 7.2$  Hz, 3H) ppm; HRMS (FAB<sup>-</sup>) [M-H]<sup>+</sup> calculated for C<sub>15</sub>H<sub>24</sub>NO<sub>3</sub>S 298.1477, found 298.1483. The NOE spectrum is given in Figure S6 of the Supporting Information.

**2,2'-(4-Methoxyphenyl)-amino-N-[(4-methylphenyl)sulfonyl]ethanol (19A).** <sup>1</sup>H NMR (400 MHz, CDCl<sub>3</sub>/TMS) = 7.72 (d,  $J = 8.4$  Hz, 2H), 7.19 (d,  $J = 8.4$  Hz, 2H), 6.75–6.95 (m, 4H), 5.26 (br, 1H), 4.33 (m, 1H), 3.50–3.80 (m, 1H), 3.73 (s, 3H), 2.36 (s, 3H) ppm; HRMS (FAB<sup>-</sup>) [M-H]<sup>+</sup> calculated for C<sub>16</sub>H<sub>18</sub>NO<sub>4</sub>S 320.0957, found 320.0948.

**2,2'-(4-Methylphenyl)-amino-N-[(4-methylphenyl)sulfonyl]ethanol (20A).** <sup>1</sup>H NMR (400 MHz, CDCl<sub>3</sub>/TMS) = 7.77 (d,  $J = 8.0$  Hz, 2H), 7.54 (d,  $J = 8.0$  Hz, 2H), 7.27 (d,  $J = 8.0$  Hz, 2H), 7.09 (d,  $J = 8.0$  Hz, 2H), 5.85 (d,  $J = 6.4$  Hz, 1H), 4.32 (q,  $J = 6.4$  Hz, 1H), 3.66 (d,  $J = 6.4$  Hz, 1H), 2.32 (s, 3H), 2.24 (s, 3H) ppm; HRMS (FAB<sup>-</sup>) [M-H]<sup>+</sup> calculated for C<sub>16</sub>H<sub>18</sub>NO<sub>3</sub>S 304.1007, found 304.1008.

**2,2'-(4-Chlorophenyl)-amino-N-[(4-methylphenyl)sulfonyl]ethanol (22A).** <sup>1</sup>H NMR (400 MHz, CDCl<sub>3</sub>/TMS) = 7.76 (d,  $J = 8.4$  Hz, 2H), 7.49 (d,  $J = 8.4$  Hz, 2H), 7.23 (d,  $J = 8.4$  Hz, 2H), 6.97 (d,  $J = 8.4$  Hz, 2H), 6.21 (d,  $J = 6.9$  Hz, 1H), 4.36 (m, 1H), 3.50–3.70 (m, 2H), 2.33 (s, 3H) ppm; HRMS (FAB<sup>-</sup>) [M-H]<sup>+</sup> calculated for C<sub>15</sub>H<sub>16</sub>ClNO<sub>3</sub>S 324.0461, found 324.0460.

**2,2'-(4-Trifluoromethylphenyl)-amino-N-[(4-methylphenyl)sulfonyl]ethanol (23A).** <sup>1</sup>H NMR (400 MHz, CDCl<sub>3</sub>/TMS) = 7.81 (d,  $J = 8.4$  Hz, 2H), 7.55 (d,  $J = 8.2$  Hz, 2H), 7.41 (d,  $J = 8.2$  Hz, 2H), 7.20 (d,  $J = 8.4$  Hz, 2H), 6.08 (d,  $J = 6.8$  Hz, 1H), 4.51 (m, 1H), 3.74 (m, 2H), 2.33 (s, 3H); HRMS (FAB<sup>-</sup>) [M-H]<sup>+</sup> calculated for C<sub>16</sub>H<sub>16</sub>NO<sub>3</sub>S 359.0803, found 358.0727.

**Computational Methodology.** All calculations were performed using the M06 functional<sup>50</sup> within the framework of unrestricted DFT. For Os, the LanL2dz basis set was<sup>51,52</sup> used with extra f polarization function,<sup>53</sup> and for all other atoms 6-31G(d) basis set<sup>54</sup> was employed. This combined basis set is denoted as BS1. Frequency calculations at the same level of theory were performed to confirm that all the optimized structures on the potential energy surface correspond to either an equilibrium structure or a transition state.<sup>55</sup> The confirmation of the transition-state structures was done by analyzing the relative movement of the transition-state geometry toward the reactant and product side of the reaction. Solvation corrections were included by single-point calculation of gas-phase optimized structures using the polarized continuum model (CPCM)<sup>54</sup> with water as a solvent, which is directly involved in the reaction. A better basis set denoted as BS2 was employed for the CPCM single-point calculation. In BS2, all atoms were treated with 6-311++G(d,p) basis set<sup>56</sup> except for Os, which was treated with the LanL2dz(f) basis set as in BS1. The solvation energy and thermal correction to the Gibbs free energy in the gas phase were used for the evaluation of the Gibbs free energy in solution. All DFT calculations were done with an ultrafine grid<sup>57</sup> using the Gaussian 09 program package.<sup>58</sup>

## ASSOCIATED CONTENT

### Supporting Information

NMR spectra, illustrated optimized geometries of intermediates and transition states, free energy diagram for aminohydroxylation, discussion of aminohydroxylation. Additional computational data, including coordinates and energies for all described stationary structures. The Supporting Information is available free of charge on the ACS Publications website at DOI: 10.1021/acs.inorgchem.5b01083.

## AUTHOR INFORMATION

### Corresponding Authors

\*E-mail: sugimoto@mls.eng.osaka-u.ac.jp. (H.S.)

\*E-mail: kazunari@ms.ifoc.kyushu-u.ac.jp. (K.Y.)

\*E-mail: shinobu@mls.eng.osaka-u.ac.jp. (S.I.)

### Notes

The authors declare no competing financial interest.

## ACKNOWLEDGMENTS

This work was supported by grants (No. 24109015, Stimuli-responsive Chemical Species and No. 22105007, Molecular activation) for Scientific Research on Innovative Areas from MEXT of Japan. Y.S. and K.Y. thank Grants-in-Aid for Scientific Research (Nos. 25410071, 24109014, and 15k13710) from the Japan Society for the Promotion of Science and the Ministry of Education, Culture, Sports, Science and Technology (MEXT) of Japan and the MEXT Projects of “Integrated Research on Chemical Synthesis” and “Elements Strategy Initiative” for their support of this work.

## REFERENCES

- Bergmeier, S. C. *Tetrahedron* **2000**, *56*, 2561–2576.
- Donohoe, T. J.; Callens, C. K. A.; Flores, A.; Lacy, A. R.; Rath, A. H. *Chem.—Eur. J.* **2011**, *17*, 58–76.
- Bestatin: (a) Umezawa, H.; Aoyagi, T.; Suda, H.; Hamada, M.; Takeuchi, T. *J. Antibiot.* **1976**, *29*, 97–99. (b) Nakamura, H.; Suda, H.; Takita, T.; Aoyagi, T.; Umezawa, H.; Iitaka, Y. *J. Antibiot.* **1976**, *29*, 102–103. (c) Bergmeier, S. C.; Stanchina, D. M. *J. Org. Chem.* **1999**, *64*, 2852–2859.
- Hapalosin: (a) Dinh, T. Q.; Du, X.; Smith, C. D.; Armstrong, R. W. *J. Org. Chem.* **1997**, *62*, 6773–6783. (b) Haddad, M.; Botuha, C.; Larcheveque, M. *Synlett.* **1999**, 1118–1120. (c) O’Connell, C. E.; Salvato, K. A.; Meng, Z.; Littlefield, B. A.; Schwartz, C. E. *Bioorg. Med. Chem. Lett.* **1999**, *9*, 1541–1546. (d) Wangner, B.; Gonzalez, G. I.; Dau, M. E. T. H.; Zhu, L. *Bioorg. Med. Chem.* **1999**, *7*, 737–747.
- Anisomycin: (a) Schaefer, J. P.; Wheatley, P. J. *J. Chem. Soc., Chem. Commun.* **1967**, 578–579. (b) Grollman, A. P. *J. Biol. Chem.* **1967**, *242*, 3226–3233. (c) Schaefer, J. P.; Wheatley, P. J. *J. Org. Soc.* **1968**, *33*, 166–169. (d) He, A.-W. R.; Cory, J. G. *Anticancer Res.* **1999**, *19*, 421–428.
- Myriocin: (a) Bagii, J. F.; Kluepfel, D.; Jacques, M., St. *J. Org. Chem.* **1973**, *38*, 1253–1260. (b) Kluepfel, D.; Bagii, J.; Baker, H.; Charest, M. P.; Kudelski, A.; Sehgal, S. N.; Vezina, C. *J. Antibiot.* **1972**, *25*, 109–115.
- Cytoxazone: (a) Kakeya, H.; Morishita, M.; Kobinata, M.; Osono, M.; Ishizuka, M.; Osada, H. *J. Antibiot.* **1998**, *51*, 1126–1128. (b) Kakeya, H.; Morishita, M.; Koshino, H.; Morita, T.; Kobayashi, K.; Osada, H. *J. Org. Chem.* **1999**, *64*, 1052–1053.
- Swainsonine: Molyneux, R. J.; James, L. F. *Science* **1982**, *216*, 190–191.
- Daunomycin: Tan, C.; Tasaka, H.; Yu, K.-P.; Murphy, M. L.; Karnofsky, D. A. *Cancer* **1967**, *20*, 333–353.
- Aceropterin: Rodrigue, A. D.; Soto, J. J. *Tetrahedron Lett.* **1996**, *37*, 2687–2690.
- Sharpless, K. B.; Patrick, D. W.; Truesdale, L. K.; Biller, S. A. *J. Am. Chem. Soc.* **1975**, *97*, 2305–2307.
- Sharpless, K. B.; Hori, T. *J. Org. Chem.* **1976**, *41*, 177–179.
- Chong, A. O.; Oshima, K.; Sharpless, K. B. *J. Am. Chem. Soc.* **1977**, *99*, 3420–3426.
- Herranz, E.; Sharpless, K. B. *J. Org. Chem.* **1978**, *43*, 2544–2548.
- Patrick, D. W.; Truesdale, L. K.; Biller, S. A.; Sharpless, K. B. *J. Org. Chem.* **1978**, *43*, 2628–2638.
- Li, G.; Chang, H.-T.; Sharpless, K. B. *Angew. Chem., Int. Ed.* **1996**, *35*, 451–454.
- Rudolph, J.; Sennhenn, P. C.; Vlaar, C. P.; Sharpless, K. B. *Angew. Chem., Int. Ed.* **1996**, *35*, 2810–2813.

- (18) Bruncko, M.; Schlingloff, G.; Sharpless, K. B. *Angew. Chem., Int. Ed.* **1997**, *36*, 1483–1486.
- (19) Kolb, H. C.; Sharpless, K. B. *Transition Metals for Organic Synthesis*, 2nd ed.; Wiley-VCH, Weinheim, Germany, 2004; Vol. 2, pp 309–336.
- (20) Masruri; Willis, A. C.; McLeod, M. D. *J. Org. Chem.* **2012**, *77*, 8480–8491.
- (21) Donohoe, T. J.; Johnson, P. D.; Helliwell, M.; Keenan, M. *Chem. Commun.* **2001**, 2078–2079.
- (22) Donohoe, T. J.; Johnson, P. D.; Cowley, A.; Keenan, M. *J. Am. Chem. Soc.* **2002**, *124*, 12934–12935.
- (23) Donohoe, T. J.; Bataille, C. J. R.; Gattrell, W.; Kloesges, J.; Rossingnol, E. *Org. Lett.* **2007**, *9*, 1725–1728.
- (24) Donohoe, T. J.; Callens, C. K. A.; Thompson, A. L. *Org. Lett.* **2009**, *11*, 2305–2307.
- (25) Harris, L.; Mee, S. P. H.; Furneaux, R. H.; Gainsford, G. J.; Luxenburger, A. J. *Org. Chem.* **2011**, *76*, 358–372.
- (26) Donohoe, T. J.; Callens, C. K. A.; Fores, A.; Mesch, S.; Poole, D. L.; Roslan, I. A. *Angew. Chem., Int. Ed.* **2011**, *50*, 10957–10960.
- (27) Donohoe, T. J.; Callens, C. K. A.; Lacy, A. R.; Winter, C. *Eur. J. Org. Chem.* **2012**, 655–663.
- (28) Pullin, R. D. C.; Rathi, A. H.; Melikhova, E. Y.; Winter, C.; Thompson, A. L.; Donohoe, T. J. *Org. Lett.* **2013**, *15*, 5492–5495.
- (29) Michaelis, D. J.; Shaffer, C. J.; Yoon, T. P. *J. Am. Chem. Soc.* **2007**, *129*, 1866–1867.
- (30) Michaelis, D. J.; Ischay, M. A.; Yoon, T. P. *J. Am. Chem. Soc.* **2008**, *130*, 6610–6615.
- (31) Michaelis, D. J.; Williamson, K. S.; Yoon, T. P. *Tetrahedron* **2009**, *65*, 5118–5124.
- (32) Williamson, K. S.; Yoon, T. P. *J. Am. Chem. Soc.* **2010**, *132*, 4570–4571.
- (33) Williamson, K. S.; Yoon, T. P. *J. Am. Chem. Soc.* **2012**, *134*, 12370–12373.
- (34) Liu, G.-S.; Zhang, Y.-Q.; Yuan, Y.-A.; Xu, H. *J. Am. Chem. Soc.* **2013**, *135*, 3343–3346.
- (35) For example, the median lethal oral dose in rats (the LD<sub>50</sub>) of OsO<sub>4</sub> (0.01 g/kg) is significantly reduced in K<sub>2</sub>[Os<sup>VI</sup>O<sub>2</sub>(OH)<sub>4</sub>] (2.69 g/kg), which has a lower oxidation state of Os(VI) than OsO<sub>4</sub>. The reduced LD<sub>50</sub> is larger than those of FeCl<sub>3</sub> (LD<sub>50</sub> = 0.09 g/kg) and CuCl<sub>2</sub> (LD<sub>50</sub> = 0.14 g/kg), indicating less toxicity of K<sub>2</sub>[Os<sup>VI</sup>O<sub>2</sub>(OH)<sub>4</sub>] than FeCl<sub>3</sub> and CuCl<sub>2</sub>.
- (36) Although K<sub>2</sub>[OsO<sub>2</sub>(OH)<sub>4</sub>] is not volatile and can be employed as a safer reagent than OsO<sub>4</sub>, its use in substrate oxidation as the precatalyst may produce volatile osmium(VIII) species with an oxidant.
- (37) Sugimoto, H.; Kitayama, K.; Mori, S.; Itoh, S. *J. Am. Chem. Soc.* **2012**, *134*, 19270–19280.
- (38) Sugimoto, H.; Ashikari, K.; Itoh, S. *Chem.—Asian. J.* **2013**, *8*, 2154–2160.
- (39) Srinivas, B.; Kumar, V. P.; Surendra, R. K.; Nageswar, Y. V. D.; Rao, K. R. *J. Mol. Catal. A: Chem.* **2007**, *261*, 1–5.
- (40) Ibuka, T.; Nakai, K.; Habashita, H.; Hotta, Y.; Otake, A.; Tamamura, H.; Fujii, N.; Mimura, N.; Miwa, Y.; Taga, T.; Chounan, Y.; Yamamoto, Y. *J. Org. Chem.* **1995**, *60*, 2044–2058.
- (41) Tiecco, M.; Testaferrri, L.; Temperini, A.; Bagnoli, L.; Marini, F.; Santi, C. *Chem.—Eur. J.* **2004**, *10*, 1752–1764.
- (42) Muñiz, K. *Chem. Soc. Rev.* **2004**, *33*, 166–174.
- (43) The products were characterized by chiral HPLC, where the column and analytical conditions were identical with those employed in chiral aminohydroxylation of methylcinnamate reported by the Sharpless method.<sup>16</sup>
- (44) Recrystallization of the isolated compound **2** resulted in precipitation of the oxido-hydroxido-osmium(V) complex.
- (45) Evans, D. F. *J. Chem. Soc.* **1959**, 2003–2005.
- (46) The smaller value of the magnetic moment than that estimated from a doublet ground state may be due to the significant spin–orbital coupling. The proton signals were broadened as found in the <sup>1</sup>H NMR spectrum of the oxido-hydroxido-osmium(V) complex.<sup>38</sup>
- (47) Winkler, J. R.; Gray, H. B. *Struct. Bonding (Berlin, Ger.)* **2012**, *142*, 17–28.
- (48) Borah, A. J.; Phukan, P. *Tetrahedron Lett.* **2014**, *55*, 713–715.
- (49) Chandrasekhar, S.; Narsihmulu, C.; Sultana, A. S. *Tetrahedron Lett.* **2002**, *43*, 7361–7363.
- (50) Zhao, Y.; Truhlar, D. G. *Acc. Chem. Res.* **2008**, *41*, 157–167.
- (51) Hay, P. J.; Wadt, W. R. *J. Chem. Phys.* **1985**, *82*, 270–283.
- (52) Hay, P. J.; Wadt, W. R. *J. Chem. Phys.* **1985**, *82*, 299–310.
- (53) Ehlers, A. W.; Bohme, M.; Dapprich, S.; Gobbi, A.; Hollwarth, A.; Jonas, V.; Kohler, K. F.; Stegmann, R.; Veldkamp, A.; Frenking, G. *Chem. Phys. Lett.* **1993**, *208*, 111–114.
- (54) (a) Ditchfield, R.; Hehre, W. J.; Pople, J. A. *J. Chem. Phys.* **1971**, *54*, 724–728. (b) Hariharan, P. C.; Pople, J. A. *Theor. Chem. Acc.* **1973**, *28*, 213–222.
- (55) Cossi, M.; Rega, N.; Scalmani, G.; Barone, V. *J. Comput. Chem.* **2003**, *24*, 669–681.
- (56) Krishnan, R.; Binkley, S.; Seeger, R.; Pople, J. A. *J. Chem. Phys.* **1980**, *72*, 650–654.
- (57) Wheeler, S. E.; Houk, K. N. *J. Chem. Theory Comput.* **2010**, *6*, 395–404.
- (58) Frisch, M. J.; Trucks, G. W.; Schlegel, H. B.; Scuseria, G. E.; Robb, M. A.; Cheeseman, J. R.; Scalmani, G.; Barone, V.; Mennucci, B.; Petersson, G. A.; Nakatsuji, H.; Caricato, M.; Li, X.; Hratchian, H. P.; Izmaylov, A. F.; Bloino, J.; Zheng, G.; Sonnenberg, J. L.; Hada, M.; Ehara, M.; Toyota, K.; Fukuda, R.; Hasegawa, J.; Ishida, M.; Nakajima, T.; Honda, Y.; Kitao, O.; Nakai, H.; Vreven, T.; Montgomery, J. A., Jr.; Peralta, J. E.; Ogliaro, F.; Bearpark, M.; Heyd, J. J.; Brothers, E.; Kudin, K. N.; Staroverov, V. N.; Kobayashi, R.; Normand, J.; Raghavachari, K.; Rendell, A.; Burant, J. C.; Iyengar, S. S.; Tomasi, J.; Cossi, M.; Rega, N.; Millam, J. M.; Klene, M.; Knox, J. E.; Cross, J. B.; Bakken, V.; Adamo, C.; Jaramillo, J.; Gomperts, R.; Stratmann, R. E.; Yazyev, O.; Austin, A. J.; Cammi, R.; Pomelli, C.; Ochterski, J. W.; Martin, R. L.; Morokuma, K.; Zakrzewski, V. G.; Voth, G. A.; Salvador, P.; Dannenberg, J. J.; Dapprich, S.; Daniels, A. D.; Farkas, O.; Foresman, J. B.; Ortiz, J. V.; Cioslowski, J.; Fox, D. J. *Gaussian 09, Revision D.01*; Gaussian, Inc.: Wallingford, CT, 2009.